Chapter 4

EFFECT OF WIND AND STRUCTURAL PARAMETERS ON ACROSS WIND LOAD OF SUPER HIGH-RISE BUILDINGS

4.1 Introduction

The design of super high-rise buildings necessitates careful consideration of wind loads, with a particular emphasis on the across-wind load, which plays a crucial role in their structural stability. However, the relationship between across-wind load and various wind and building parameters remains unclear. In this chapter, we aim to investigate and quantify the impact of wind and structural parameters on the across-wind load of super high-rise buildings within a practical range. Out of structural parameters, the Natural frequency of the structure (f) and structural damping ratio (ζ_s) are selected due to their key role in the calculation of across wind load. Four parameters (Exponent of mean velocity profile (α), turbulence intensity (I_H), peak factor for resonant response (g_R), and the background peak factor (g_B)) are selected out of wind parameters because of their significance in defining the characteristics of wind approaching the structure. Thus, the effects of these parameters on the across wind load are examined in this chapter. A hypothetical 300 m super high-rise building with a square cross-section, assumed to be located in urban terrain, is adopted for the analysis.

In order to comprehend the range of parameters, several international codes are used for each parameter evaluation. For suitability, we have referred to the codes that explicitly provided the corresponding parameters. Various international codes/ Standards have provided certain values of these parameters applicable to their specific site conditions. An understanding of how these parameters affect the across wind load will greatly assist engineers in accurately calculating the across-wind load for the structure. Accurate estimation of wind and structural parameters is essential because inaccurate estimation of these parameters will lead to underestimation or overestimation of across wind load. An incorrect load calculation will result in a faulty building design.

4.2 Fixed parameters of the building

This research investigates a theoretical tall structure located within the city environment. The wind direction and the plan of the building are shown in Figure (3.1). The plan dimension, height & other parameters of the building which are kept constant throughout this study are enumerated in Table 4.1. A discussion of the parameters which are varied will follow in the next section.

Table 4.1 Building parameters that are kept constant throughout the study

H(m)	B(m)	D(m)	β	M^*_1(kg)
300	50	50	1	5.0 x10^7

4.3 Structural parameters

4.3.1 Natural frequency of the structure (*f*)

When it comes to determining wind loads, the natural period of a building holds the utmost importance. Table 4.2 shows the formulations available to calculate time period (T) of tall RC buildings for wind design. The natural frequency of high-rise buildings with a height of H meter would be $f_1 = \frac{1}{T_1}$.

Natural time period is calculated according to the various codal provisions. There exists wide variability in the expressions for natural period provided by different codes and researchers. It is clearly visible from Table 4.2 that only Indian standard takes into account the base dimension in the formulation of time period. All other expressions are function of total height of the building only.

Table 4.2 Various recommendation of natural period [See Figure (3.1) for H & D]

Code	Natural Time Period (T)	Natural Frequency (f)
ASCE 7-2016	$T = H^{0.9}/43.5$	0.2565
Eurocode 2005	$T = 0.022H$	0.1515
Ha *et al.* (2020)	$T = 0.0196H$	0.1700
IS 875 (Part 3): 2015	$T = 0.09H/\sqrt{D}$	0.2619
KBC 2009	$T = 0.073H^{0.75}$	0.1900
Lagomarsino (1993)	$T = 0.018H$	0.1852
Tamura (2000)	$T = 0.015H$	0.2222

4.3.2 Structural damping ratio (ζ_s)

From the perspective of structural response under dynamic loading, structural damping is a crucial parameter. Table 4.3 lists the various structural damping ratios of the numerous codal provisions.

Table 4.3 Structural damping ratios of tall RC building

Code	Structural damping ratio(ζ_s)
ASCE 7-2016	2%
AS/NZ1170: 2011	1%
Eurocode 2005	1.57%
ISO 2009	1.2%
IS 875 (Part 3): 2015	2%

4.4 Wind parameters

4.4.1 Exponent of mean velocity profile (α)

Exponent of mean velocity profile(α) is a pivotal parameter in defining the approaching wind profile. Equation (4.1) shows the power-law profile of approaching wind.

$$U(H) = U_{ref}\left(\frac{H}{H_{ref}}\right)^{\alpha} \tag{4.1}$$

Where, U_H is the wind speed at height H, H_{ref} is the reference height taken as 10 meters. U_{ref} is called as reference wind speed which is defined at the reference height. In this case U_{ref} is considered as 25.2326 m/s. H_{ref} and U_{ref} are kept constant, and only exponent of mean wind velocity (α) is varied. Various international standards recommend the values of exponent of mean velocity profile for different types of terrain categories. The value of α and wind speed for the urban terrain are shown in Table 4.4.

Table 4.4 Exponent of mean velocity profile for urban terrain

Code	Exponent of mean velocity profile for urban terrain (α)	Wind speed at the Tip of target building (U_H) in m/s
AIJ 2004	0.35	82.98
ASCE 7-2016	0.25	59.05
GB 50009: 2012	0.30	70
ISO 2009	0.40	98.36
NBCC 2020	0.36	85.84

4.4.2 Turbulence intensity (I_H)

Turbulence intensity gives an understanding of wind turbulence in the approaching flow and it affects the effective wind loads on the structure. International codes have provided formulations to assess the turbulence intensity at the location of the building based on the terrain category parameters as presented in Table 4.5.

Table 4.5 Turbulence intensity profile and its parameters for urban terrain

Code	Turbulence intensity for urban terrain	Different parameters and their values for urban terrain	Turbulence Intensity in Percentage
ASCE 7-2016	$I_z = c\left(\frac{10}{\bar{z}}\right)^{1/6}$	c=0.30, $\bar{z} = 0.6h$	18.53
AS/NZ 1170 :2011(formulated)	$I_z = c\left(\frac{10}{\bar{z}}\right)^{d}$	c=0.40, d=0.24	17.68
Eurocode 2005	$I_z = \left(\frac{1}{ln(z/z_0)}\right)$	z_0=1, z=h	17.53
IS 875 (Part 3): 2015	$I_{z,4} = 0.466 - 0.1358 log_{10}\left(\frac{z}{z_{0,4}}\right)$	$z_{0,4}$ = 2, z=h	17
ISO 2009	$I_z = \left(\frac{1}{ln(z/z_0)}\right)$	z_0=3, z=h	21.71

4.4.3 Peak factor for resonant response (g_R)

The peak factor for resonant response (g_R) is influenced by the averaging time (T) and the up-crossing rate (v), which is nearly equivalent to the natural frequency of the structure under the assumption that the development is narrow banded Gaussian. Quan and Gu (2012) used the peak factor related to averaging time 10-minutes (600 sec), so here, for the conformity, we have opted the international standards, which specifically use 10-min averaging time. Here, f_1 is fundamental natural frequency of the building. Quan and Gu (2012) used the fundamental frequency as 0.2 Hz so for comparison of different peak background factor, fundamental frequency is kept constant as 0.2 Hz for all cases. Various codal provisions for estimating the peak factor for resonant response are presented in Table 4.6.

Table 4.6. Peak factor for resonant response for various codes and its magnitude at fundamental frequency 0.2 Hz

Code	Peak factor for resonant response (g_R)	f = 0.20 Hz
AIJ 2004	$g_R=\sqrt{2\ln(600f_1)+1.2)}$	3.2825
AS/NZ 1170: 2011	$g_R=\sqrt{2\ln(600f_1)}$	3.0943
Eurocode 2005	$g_R=\sqrt{2\ln(600f_1)}+\frac{0.6}{\sqrt{2\ln(600f_1)}}$	3.2882
ISO 2009	$g_R=\sqrt{2\ln(600f_1)}+\frac{0.577}{\sqrt{2\ln(600f_1)}}$	3.2808
GB 50009: 2012	2.5	2.5

4.4.4 Background peak factor (g_B)

Almost all codes use a single value for the background peak factor. The Japanese and European codes use the value of g_B same as g_R. Table 4.7 shows the background peak factors adopted from various codal provisions. In contrast to other codes, the Chinese code specifies a fixed value of 2.5 for g_B and g_R, leading to significantly lower values.

Table 4.7 Various codal recommendation for Background Peak factor

Code	Background Peak factor (g_B)
AIJ 2004	$g_B = g_R$ =3.2825
AS/NZ 1170: 2011	3.7
Eurocode 2005	$g_B = g_R$ =3.2882
ISO 2009	3.4
GB 50009: 2012	2.5

4.5 Methodology

Following the instructions of the Section (3.4), a MATLAB (Appendix A) code is developed in the present study to evaluate all the parameters and compute the across wind ESWL and responses. The validation of the code is done by comparing the results with Quan and Gu (2012) as shown in Fig. 3.2. The evaluation of parameters is conducted using provisions of international codes in order to understand the range of parameters then the evaluated parameters are used in the formulation. There is a total of six parameters, whose effect on across wind load is studied. Out of six parameters, only one is varied at a time, while the other independent parameters are kept constant. Table 4.8 contains the fixed values of parameters. The effect of each parameter on across wind load and response is analysed.

Table 4.8 Fixed value of parameters.

Parameter	Value
Natural frequency(f) of the structure	0.20 Hz
Structural damping ratio (ζ_s)	1%
Exponent of mean velocity profile (α)	0.30
Turbulence intensity (I_H)	11%
Peak factor for resonant response (g_R)	3.281
Background peak factor (g_B)	3.5

4.6 Results and Discussion

4.6.1 Effect of natural frequency (*f*) of the structure

The across wind load of the super high-rise building is calculated on different natural frequencies. Table 4.8 lists the parameters that are kept constant in this section. The provisions for determining natural frequencies according to various codes are presented in the section structural parameters. The calculation procedures for calculating the across-wind ESWL and response are succinctly discussed in the Section (3.4) Systematic computation steps to calculate across wind ESWL. Figures 4.1 (a)-(d) show the variation in ESWL, shear force, bending moment, and peak acceleration along the height of the building. Peak factor for resonant response (g_R) is dependent on fundamental natural frequency of the structure. Therefore, g_R is automatically varied while varying the natural frequency in this case. The parameters other than these two are kept constant. The Eurocode 2005 proposes the lowest natural frequency for the building, while IS 875 (Part 3): 2015 recommends the highest. As per the Figure 4.1, it is evident that the results obtained are maximum for Eurocode 2005, while the results for IS 875 (Part 3): 2015 are the minimum. It is evident from the results that as the natural frequency of the building is decreasing, the across wind load and responses are increasing. It is happening because the background components are highly sensitive to reduced frequency (n) which is a function of natural frequency. In order to facilitate the discussion, the mean value of wind load and responses for all the codes are calculated. The percentage difference from mean is calculated as:

*Percentage difference from mean = [(Present codal value - Mean Value)/Mean value]*x*100*

Where, present codal value is the notation used for the calculated parameter from the particular code. Fig. 4.2 depicts the variation of wind load and response from the mean value of all the codes. KBC 2009 & Logomarsino 1993 have percentage difference 2.94 & 7.39 respectively, which are close to the mean value. Eurocode 2005 is 54.30% higher than mean value and ASCE 7-2016 is 33.76% lower than mean value.

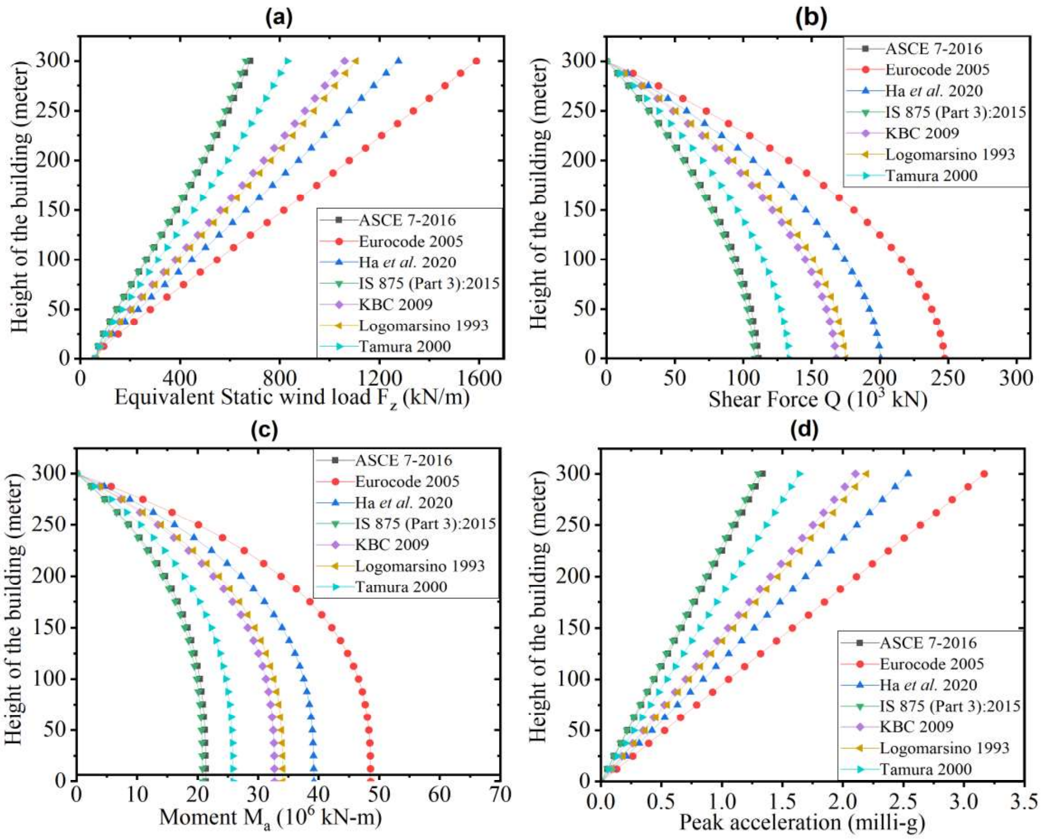

Figure 4.1 ESWL, Shear Force, Moment and Peak acceleration along the height of the building for various natural frequencies

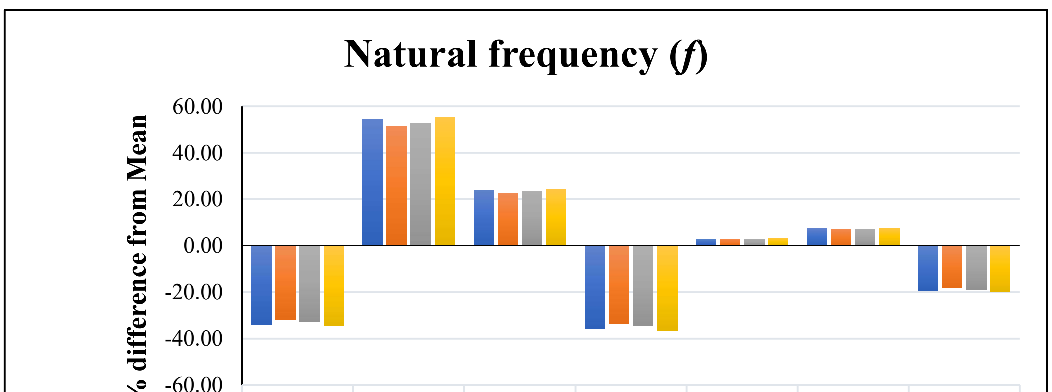

	ASCE 7-2016	Eurocode 2005	Ha et al. 2020	IS 875 (Part 3):2015	KBC 2009	Logomarsino 1993	Tamura 2000
ESWL	-33.76	54.30	23.96	-35.51	2.94	7.39	-19.32
Shear Force	-31.88	51.28	22.62	-33.53	2.78	6.98	-18.25
Bending Moment	-32.80	52.75	23.27	-34.49	2.86	7.18	-18.77
Peak Acceleration	-34.46	55.22	24.45	-36.26	3.08	7.61	-19.64

Figure 4.2 Percentage difference from mean values of ESWL, Shear force, Bending moment & peak acceleration for varying natural frequencies.

4.6.2 Effect of structural damping ratio (ζ_s)

In this section, the across wind load is calculated at different structural damping ratio (ζ_s) and keeping all the other parameters constant. As mentioned in Table 4.3, AS/NZ 1170: 2011 recommends the lowest value of the structural damping ratio of the building, while ASCE 7-2016 and IS 875 (Part 3): 2015 suggest the highest value. Figures 4.4 (a) -(d) delineate the variation of ESWL, shear force, bending moment, and peak acceleration along the building height. It can be observed from Figures 4.4 (a)-(d) that AS/NZ 1170: 2011 gives the maximum wind load. Since both ASCE 7-2016 and IS 875 (Part 3): 2015 recommend the same, and higher value of structural damping ratio, the across wind load is similar and minimum. A conclusion can be drawn that as the structural damping ratio increases the across wind load decreases. This study's findings agree with Wang *et al.* (2022) and Li *et al.* (2018), which found a decrease in cross-wind response as structural damping increased. In Figure 4.3, the fluctuations of wind load and response from the mean value of all the codes are illustrated. Figure 4.3 shows that Australian code exceeds 16% from the mean value of all the code. Eurocode 2005 is nearest to the mean value.

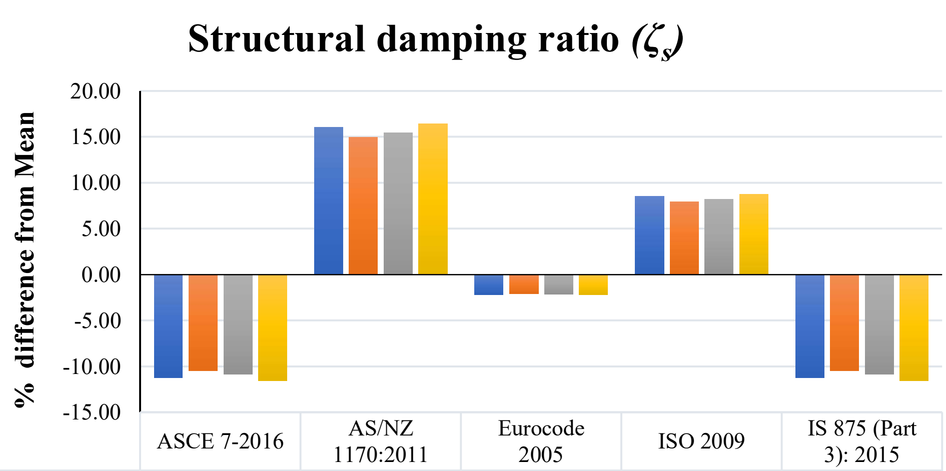

	ASCE 7-2016	AS/NZ 1170:2011	Eurocode 2005	ISO 2009	IS 875 (Part 3): 2015
ESWL	-11.20	16.01	-2.13	8.52	-11.20
Shear Force	-10.44	14.93	-1.99	7.94	-10.44
Bending Moment	-10.81	15.45	-2.06	8.22	-10.81
Peak Acceleration	-11.50	16.43	-2.18	8.75	-11.50

Figure 4.3 Percentage difference from mean values of ESWL, Shear force, Bending moment & peak acceleration for varying structural damping ratio.

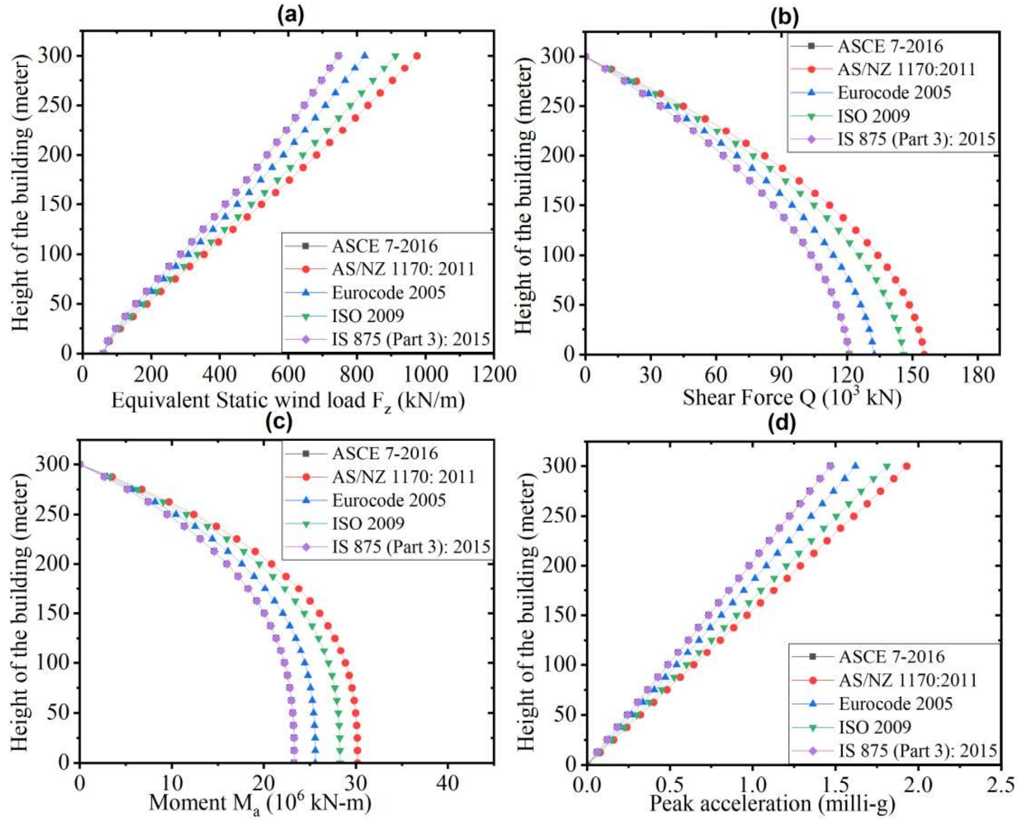

Figure 4.4 ESWL, Shear Force, Moment and Peak acceleration along the height of the building for various structural damping ratio

4.6.3 Effect of exponent of mean velocity profile (α)

Figure 4.5 (a)-(d) illustrates the impact of wind velocities provided in Table 4.4 on the across wind loads and responses. Across wind load is maximum for ISO 2009 because it has the maximum exponent value and due to this, it proposes the maximum wind velocity at height of target building. ASCE 7-2016 proposes the minimum value of exponent among other codes; hence the across wind load is minimum in this case. Based on Figure 4.5 the conclusion can be drawn that as the wind speed increases across wind load and response also increases. Gu *et al.* (2022) also concluded the same in their study. According to their statement, the susceptibility of the across-wind response is greater to the approaching wind speed as compared to the along-wind response. In general, longitudinal wind loads are more prominent at lower wind velocities, whereas transverse

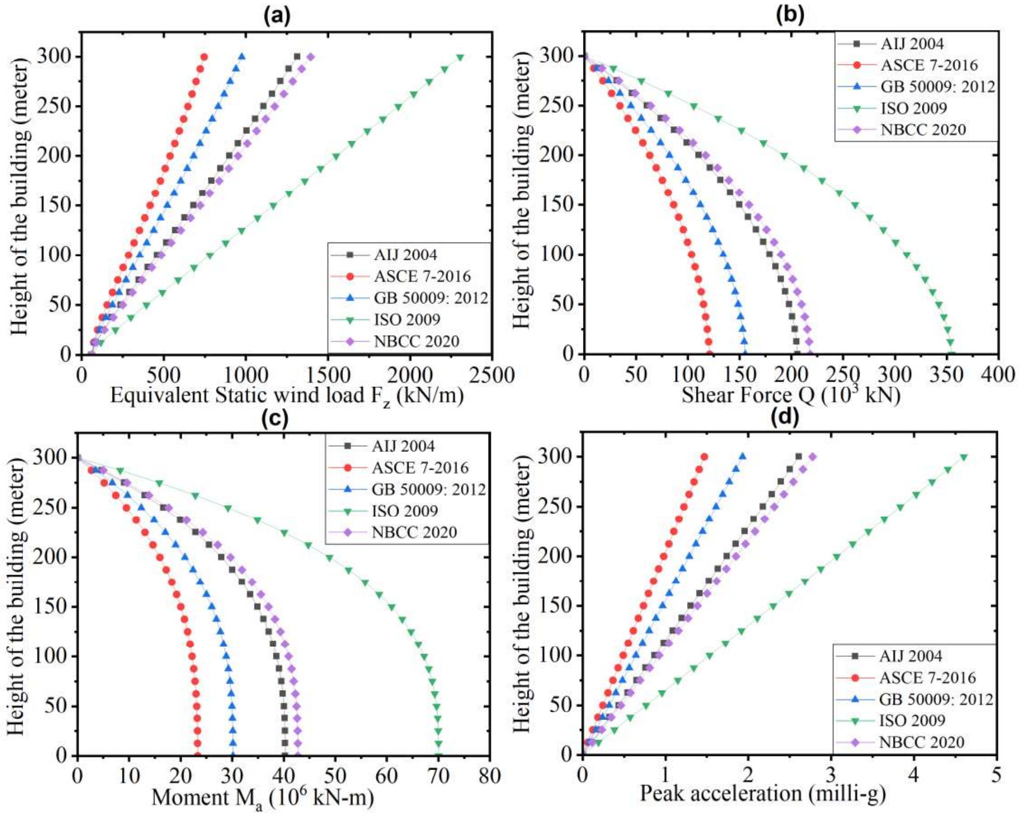

Figure 4.5 ESWL, Shear Force, Moment and Peak acceleration along the height of the building for various exponent of mean velocity profile

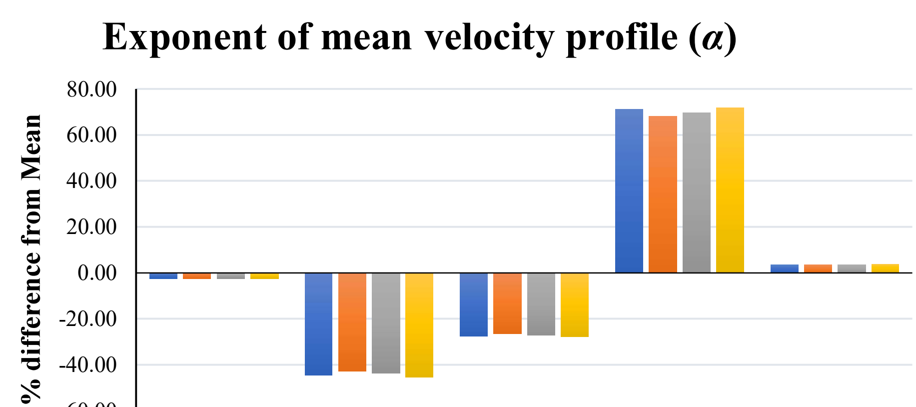

	AIJ 2004	ASCE 7-2016	GB 50009: 2012	ISO 2009	NBCC 2020
ESWL	-2.48	-44.58	-27.57	71.10	3.53
Shear Force	-2.38	-42.66	-26.38	68.04	3.38
Bending Moment	-2.43	-43.60	-26.96	69.54	3.45
Peak Acceleration	-2.44	-45.18	-27.85	71.83	3.65

Figure 4.6 Percentage difference from mean values of ESWL, Shear force, Bending moment & peak acceleration for varying exponent of mean velocity profile.

wind loads are predominant at higher velocities. The inherent frequencies of exceptionally tall structures are comparatively low, and the velocity of wind is greater at the uppermost tiers of the boundary layer. Consequently, the reduced frequency of a skyscraper at the wind speed for which it was designed may correspond to the reduced frequency at which the maximum force spectrum across the wind direction transpires. AIJ 2004 and NBCC 2020 are near to the mean value, ISO 2009 exceeds 71.83% from the mean in peak acceleration (Figure 4.6).

4.6.4 Effect of turbulence intensity (I_H)

This section involves the calculation of the across wind load of tall building at different turbulence intensity values while keeping the other five parameters constant. Through the results obtained in the study, it can be inferred that turbulence intensity has a minimal effect on the across wind loads. The results collected from the various turbulence intensities produced similar outcomes. Table 4.9 exhibits the across wind load values (kN/m) from the analysis of five international codes. Cheng *et al.* (1992) have previously deduced that the lift coefficient, an indicator of the across wind load, does not exhibit a correlation with changes in turbulence intensity. The current study has corroborated these findings. While the along-wind force spectrum primarily reflects the wind turbulence approaching the structure, the across-wind force spectrum is mostly influenced by vortex formation and flow separation. Therefore, the turbulence intensity has minimal impact on the across-wind response.

4.6.5 Effect of peak factor for resonant response (g_R)

The study analysed the across wind loads of a super high-rise building at various peak factors for resonant response (g_R) while holding the other five parameters constant (as shown in Table 8). The results were visualized in Figure 4.7 (a)-(d), which displayed the variation of

Table 4.9 Across wind ESWL of a 300 m super high-rise building at various turbulence intensity

Height of the building In meter	ASCE 7-2016	AS/NZ1170: 2011	Eurocode 2005	IS 875 (Part 3): 2015	ISO 2009
0.00	60.54	60.54	60.54	60.54	60.54
12.50	77.98	77.98	77.99	77.99	77.98
25.00	110.16	110.17	110.17	110.18	110.15
37.50	147.89	147.90	147.91	147.92	147.88
50.00	187.96	187.98	187.98	188.00	187.94
62.50	229.20	229.22	229.22	229.24	229.17
75.00	271.08	271.10	271.11	271.13	271.05
87.50	313.31	313.34	313.34	313.37	313.27
100.00	355.68	355.72	355.72	355.76	355.64
112.50	398.05	398.09	398.10	398.13	398.00
125.00	440.28	440.32	440.33	440.37	440.23
137.50	482.25	482.30	482.31	482.35	482.19
150.00	523.86	523.91	523.92	523.97	523.80
162.50	565.02	565.07	565.08	565.14	564.95
175.00	605.63	605.69	605.71	605.76	605.56
187.50	645.65	645.71	645.73	645.79	645.57
200.00	685.02	685.09	685.10	685.17	684.94
212.50	723.72	723.79	723.81	723.88	723.63
225.00	761.76	761.83	761.85	761.92	761.66
237.50	799.15	799.23	799.25	799.33	799.05
250.00	835.98	836.06	836.08	836.16	835.87
262.50	872.34	872.43	872.45	872.53	872.22
275.00	908.38	908.48	908.50	908.59	908.26
287.50	944.31	944.41	944.43	944.53	944.18
300.00	980.37	980.47	980.50	980.60	980.24

ESWL, shear force, bending moment, and peak acceleration along the height of the building. The findings from AIJ 2004, ISO 2009, and Eurocode 2005 were quite similar. However, GB 50009: 2012 showed the lowest across wind loads, primarily due to the lowest value of the resonant factor. It is observed that as the resonant factor increased, the across wind load also increased. Figure 4.8 shows the percentage difference from the mean, Eurocode 2005 exceeds 6.44% from the mean in case of peak acceleration. AS/NZ 1170: 2011 shows results similar to mean value of all the codes.

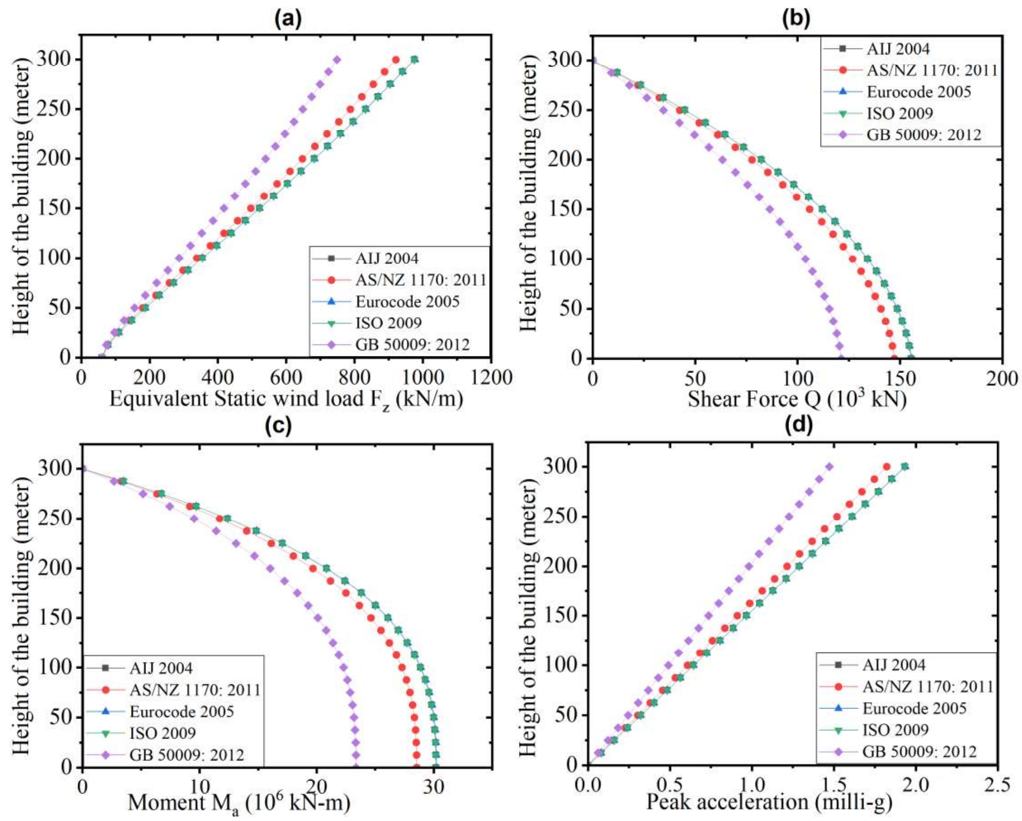

Figure 4.7 ESWL, Shear Force, Moment and Peak acceleration along the height of the building for various g_R

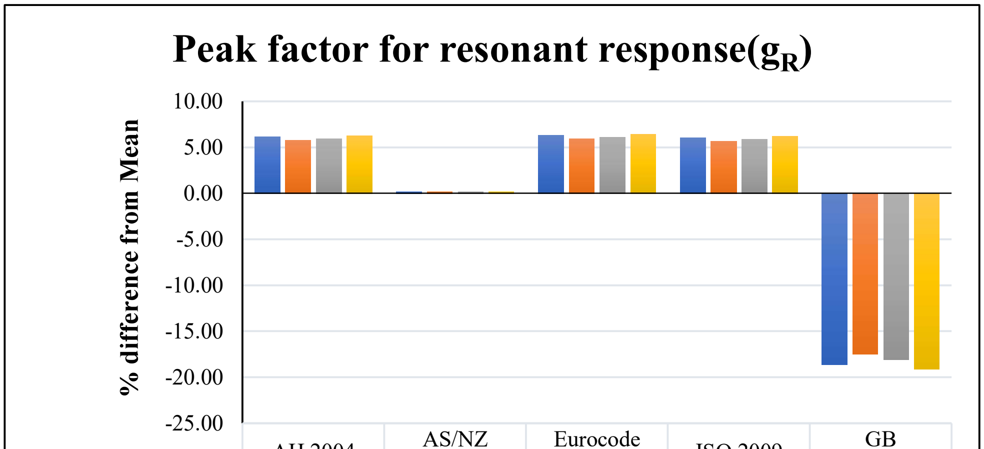

	AIJ 2004	AS/NZ 1170:2011	Eurocode 2005	ISO 2009	GB 50009:2012
ESWLat top	6.11	0.15	6.29	6.06	-18.62
Shear Force	5.73	0.14	5.90	5.68	-17.47
Bending Moment	5.92	0.15	6.09	5.87	-18.02
Peak Acceleration	6.26	0.17	6.44	6.20	-19.07

Figure 4.8 Percentage difference from mean values of ESWL, Shear force, Bending moment & peak acceleration for varying peak factor for resonant response.

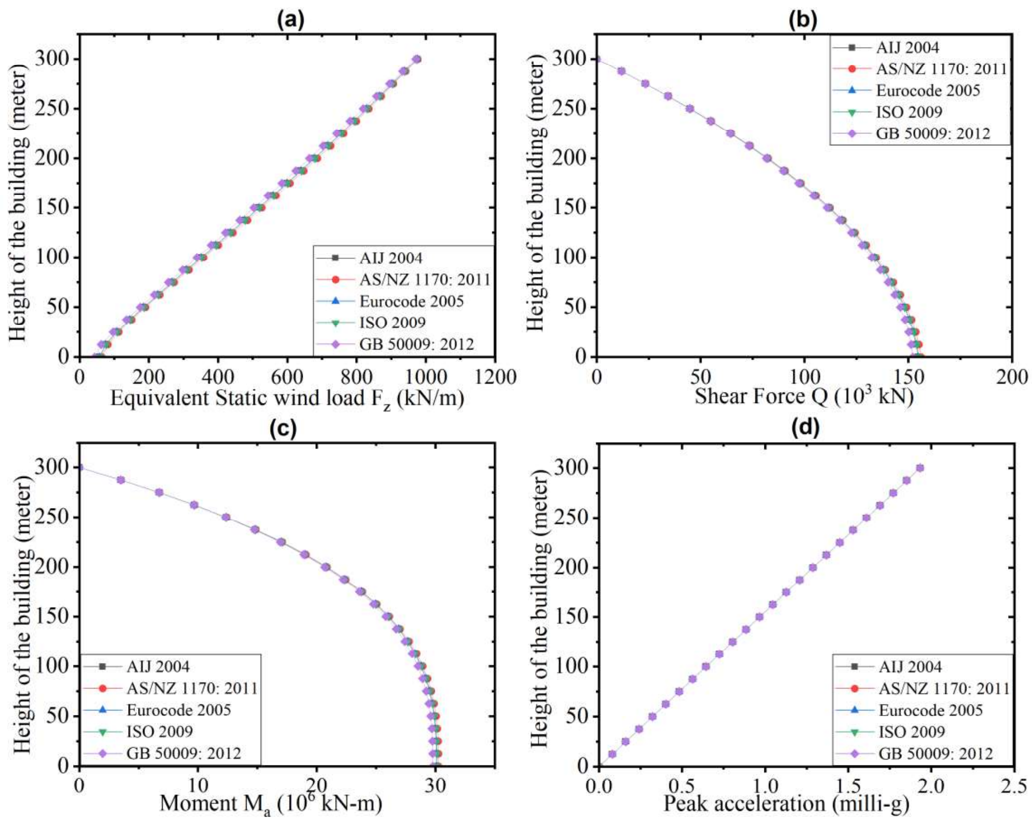

Figure 4.9 ESWL, Shear Force, Moment and Peak acceleration along the height of the building for various g_B

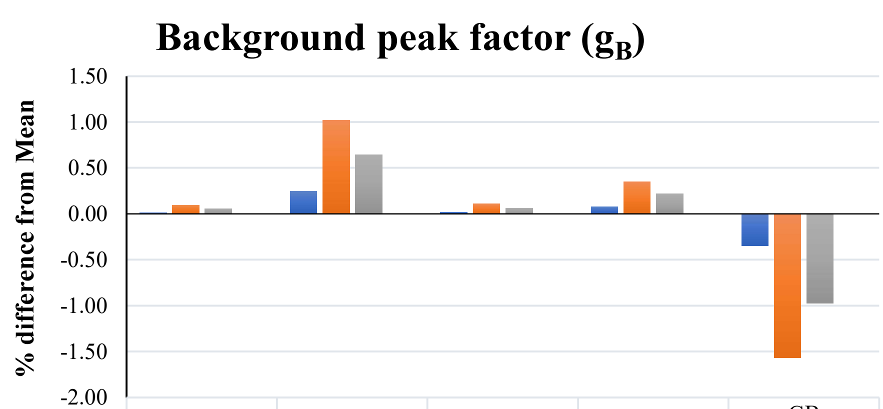

	AIJ 2004	AS/NZ 1170:2011	Eurocode 2005	ISO 2009	GB 50009:2012
ESWL	0.01	0.24	0.02	0.07	-0.35
Shear Force	0.09	1.01	0.11	0.35	-1.56
Bending Moment	0.05	0.64	0.06	0.22	-0.97
Peak Acceleration	0	0	0	0	0

Figure 4.10 Percentage difference from mean values of ESWL, Shear force, Bending moment & peak acceleration for varying background peak factor.

4.6.6 Effect of background peak factor (g_B)

The background response refers to a type of quasi-static response that occurs by variations in turbulence wind at low frequencies, which are too low to instigate any resonant response (Holmes 2001). This section examines the across wind loads of the structure calculated at different background peak factor (g_B) and keeping the other five parameters constant. It can be seen from Figure 4.9(a)-(c) that effect of background peak factor on across wind load is minimum. Peak acceleration does not depend on the background peak factor (Equation (3.43)). Therefore in Figure 4.9(d), all the codes produce equal peak acceleration. Figure 4.10 shows the percentage difference from the mean, GB 50009:2012 shows 1.56% less value from the mean in case of bending moment.

4.6.7 Variations in the across wind load caused by various parameters

Figure 4.11 illustrates the variation of different parameters with the maximum across wind Equivalent Static Wind Load (ESWL), while maintaining a constant vertical axis for ESWL. The findings indicate that as the natural frequency increases, there is a rapid decrease in across wind load, highlighting the importance of higher natural frequencies for reducing wind-induced forces. Additionally, an increase in the structural damping ratio results in lower across wind load, suggesting that higher damping mitigates wind forces. The exponent of the mean velocity profile has a significant impact, showing an exponential increase in across wind load as it increases. Surprisingly, turbulence intensity does not notably influence the across wind load. Moreover, higher peak factors for resonant response and background peak factors lead to increased across wind load, emphasizing their role in amplifying wind-induced forces. Overall, the exponent of the mean velocity profile stands out as the most influential parameter affecting across wind load, underscoring its critical importance in determining wind forces on the structure.

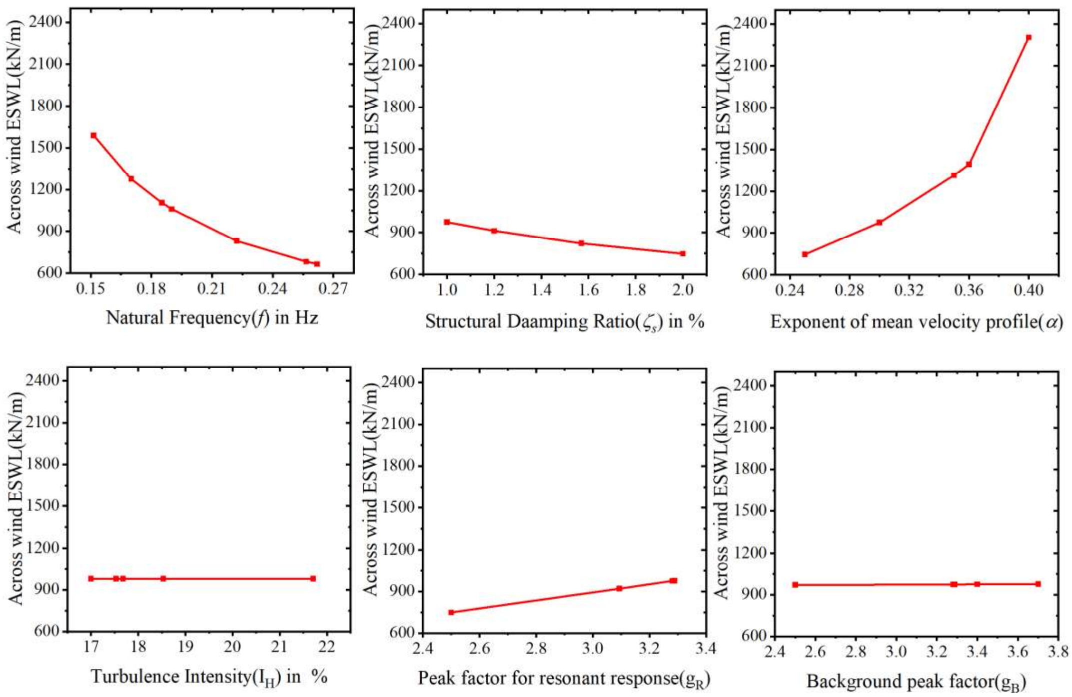

Figure 4.11 Variation of across wind load with various parameters

4.7 Concluding remarks

In conclusion, this study delves into the critical aspect of across-wind load assessment in the design of super high-rise buildings. By meticulously investigating the influence of wind and structural parameters on the across wind load, the research presents valuable insights for practitioners and engineers engaged in such architectural endeavours. The findings notably underscore the significance of the natural frequency of the structure, which dictates the responsiveness of the building to varying wind conditions. Moreover, the exponent of mean velocity profile (α) emerges as the most dominant parameter impacting cross-wind loads, highlighting its pivotal role in wind-induced effects on high-rise structures. Furthermore, the investigation highlights the relevance of the structural damping ratio in the mitigation of cross-wind loads. Higher damping ratios yield notable reductions in the across-wind ESWL, offering a promising avenue for improving building resilience. Noteworthy is the minimal impact of turbulence intensity on the across-wind load, signifying its relative insignificance in comparison to other influential parameters. Additionally, the study draws attention to the pronounced influence of peak factors, particularly g_R, on the magnitude of across-wind ESWL. This finding underscores the necessity of precise consideration of such factors in load calculations for accurate and robust high-rise building designs.

The implications of these outcomes are profound for structural engineering practices, emphasizing the indispensability of meticulous assessments of wind and structural parameters in designing super high-rise buildings. By avoiding overestimation or underestimation of wind loads, erroneous design decisions can be averted, ensuring optimal safety and structural integrity.

However, it is imperative to acknowledge certain limitations. The study relies on a hypothetical super high-rise building with specific assumptions, which may not fully capture the complexities encountered in real-world scenarios. As such, future investigations should incorporate more diverse building geometries, terrains, and meteorological conditions to enhance the generalizability of the findings. In conclusion, this research offers significant advancements in understanding the variation of wind loading in the context of super high-rise structures. Building upon these insights, it is recommended to conduct wind tunnel studies and full-scale experiments to validate and expand upon the present findings. Through the amalgamation of experimental data and computational analyses, the field of high-rise architecture can evolve with enhanced precision and resilience, mitigating potential hazards associated with across-wind loads and paving the way for safer and more sustainable super high-rise buildings in urban landscapes.